PHYSICAL REVIEW D **73,** 024001 (2006)

# Midpoint rule as a variational-symplectic integrator: Hamiltonian systems

J. David Brown

*Department of Physics, North Carolina State University, Raleigh, North Carolina 27695 USA*

(Received 9 November 2005; published 4 January 2006)

Numerical algorithms based on variational and symplectic integrators exhibit special features that make them promising candidates for application to general relativity and other constrained Hamiltonian systems. This paper lays part of the foundation for such applications. The midpoint rule for Hamilton's equations is examined from the perspectives of variational and symplectic integrators. It is shown that the midpoint rule preserves the symplectic form, conserves Noether charges, and exhibits excellent long-term energy behavior. The energy behavior is explained by the result, shown here, that the midpoint rule exactly conserves a phase space function that is close to the Hamiltonian. The presentation includes several examples.

DOI: 10.1103/PhysRevD.73.024001 PACS numbers: 04.25.Dm

## I. INTRODUCTION

This is the first in a series of papers that explore the possible advantages of using variational and symplectic numerical integration techniques for constrained Hamiltonian systems. A constrained Hamiltonian system is the Hamiltonian formulation of a gauge theory [1]. For such a theory the canonical momenta, defined by the derivatives of the Lagrangian with respect to the velocities, are not invertible for the velocities as functions of the coordinates and momenta. As Dirac showed [2], this implies the presence of constraints among the coordinates and momenta. The constraints are the canonical generators of the gauge symmetry. They appear in the action as part of the Hamiltonian, accompanied by undetermined multipliers.

Constrained Hamiltonian systems are common in physics. Examples include electrodynamics, Yang-Mills theories, string theory, and general relativity. The numerical integration of Maxwell's equations for electrodynamics has been well studied. For example, with the finite difference time domain (FDTD) method, the electric and magnetic fields are evolved using discrete forms of Ampere's and Faraday's laws [3]. The FDTD discretization automatically preserves the two Gauss's law constraints in the source free case. Yang-Mills and string theories are primarily used to describe elementary quantum systems, so for these theories the classical solutions do not play a critical role. Correspondingly, numerical methods for evolving the classical Yang-Mills fields and classical strings have not been thoroughly explored.

The most challenging example of a constrained Hamiltonian system, and the one that serves as my primary motivation for this investigation, is general relativity. There is currently a great deal of interest in developing numerical methods for solving Einstein's equations. This interest is driven by recent advances on the experimental front. A number of ground-based gravitational wave detectors are in operation today, and during the next decade some of these instruments will reach the level of sensitivity needed to detect black hole collisions. The LISA project is a joint effort between NASA and ESA, with the goal of placing a gravitational wave detector in solar orbit. The LISA detector will be capable of sensing, among other sources, collisions between the supermassive black holes that reside at the centers of galaxies. To maximize the scientific payoff of these instruments we need a theoretical understanding of the gravitational-wave signals produced by black hole collisions and other astrophysical phenomena. The only known method for predicting the gravitational wave signature of colliding black holes is through numerical simulation.

Numerical relativity is not a mature field. Researchers have spend much time and effort in developing numerical relativity codes, but the complexity of the Einstein equations coupled with the topological issues that arise when modeling black holes have made progress slow. Current codes can succeed in simulating at most about one orbit of a binary black hole system before errors completely spoil the results [4]. The main difficulty appears to be the presence of "constraint violating modes" [5–8]. These are solutions of the Einstein evolution equations that are unphysical in that they do not respect the constraints. Although the evolution equations preserve the constraints at an analytical level, numerical errors inevitably excite these constraint violating modes. Some of these modes grow exponentially fast and spoil the numerical results. What is needed for numerical relativity is an algorithm that will keep the constraints satisfied, or nearly satisfied, during the course of the evolution. It might be possible to develop a scheme like the FDTD method of electrodynamics, but the complexity and nonlinearity of the Einstein equations makes this a difficult task. Some progress along these lines has been made by Meier [9].

In this paper I begin to explore a different route for keeping the constraints satisfied for general relativity and other constrained Hamiltonian systems. The idea is based on the use of variational integrators (VI). In the traditional approach to numerical modeling by finite differences, the

 

continuum equations of motion are discretized by replacing derivatives with finite difference approximations. In the VI approach we first discretize the action, then derive the discrete equations of motion by extremizing the action. This approach was pioneered by a number of researchers beginning in the 1960's; for a brief historical overview, see Ref. [10]. Variational integrators have been developed further in recent years by Marsden and collaborators [10,11].

One of the key properties of variational integrators is that they are symplectic. This means that the discrete time evolution defined by the VI equations automatically conserves a symplectic form. The subject of symplectic integrators is well-developed; for an overview, see Ref. [12]. Variational integrators also conserve the charges associated with symmetries via Noether's theorem. For our present purposes, the most interesting characteristic of variational and symplectic integrators is their behavior regarding energy. Although these integrators do not typically conserve energy, they exhibit excellent long-time energy behavior. For other integrators the energy errors typically increase unboundedly in time. For variational and symplectic integrators the energy error is typically bounded in time.

There are various ways that one can develop a variational integrator for constrained Hamiltonian systems. For example, one can extremize the action while keeping the undetermined multipliers fixed. In that case the constraints will not remain zero under the discrete time evolution. But there is reason to believe that in many cases the constraint errors, like energy, will remain bounded in time [13]. Another option is to extremize the action with respect to the undetermined multipliers as well as the canonical coordinates and momenta. This is the most attractive approach from a number of perspectives. In this case the discrete constraints are imposed as equations of motion at each timestep, so they are guaranteed to hold under the discrete time evolution. The trade off is that the undetermined multipliers of the continuum theory are actually determined by the discrete equations of motion.

In general relativity the constraints cannot be solved for the multipliers unless the coordinates and momenta are chosen appropriately. The traditional choice of canonical coordinates [14], the spatial metric, leads to generically ill-defined equations for the multipliers. Recently Pfeiffer and York [15,16] have rewritten the constraints using the conformal metric and the trace of the extrinsic curvature as coordinates. They show that the resulting equations for the multipliers are generically well-defined. In Ref. [17] I rewrote the action and evolution equations in terms of these new coordinates and their conjugate momenta. This is one form of the action that is suitable for the development of a variational integrator for general relativity.

The essential idea of using a discrete action to define a set of discrete equations of motion that both respect the constraints and determine the multipliers has also been studied in the context of general relativity by Di Bartolo, Gambini, and Pullin [18–23]. They refer to their approach as ''consistent discretization''. They discuss consistent discretization in the context of numerical relativity, and also as a route toward quantization. There are a number of technical differences between the works of Di Bartolo, Gambini, and Pullin and the results presented in this and the following papers. The most important difference between my approach and theirs is a difference in techniques used to generate the equations of motion. I extremize the discrete action directly while Di Bartolo *et al.* identify the discrete Lagrangian as the generator of a Type 1 canonical transformation. With direct extremization we obtain useful information about the system encoded in the endpoints of the varied action. This is the key to proving the important properties of the variational integrator including symplecticity, Noether's theorem, and the good long-time behavior of energy.

In this first paper I focus on simple mechanical systems with no constraints. This is a rich subject that has been explored rather thoroughly, in mathematically precise language, by Marsden *et al.* [10,11]. The purpose of this paper is to present the key results on variational integrators in the context of a particular discretization using language familiar to most physicists. The particular discretization of the action considered here leads to the midpoint rule applied to Hamilton's equations. The midpoint rule is an old, familiar numerical algorithm. It is presented here in a new, perhaps unfamiliar light as a variational-symplectic integrator. This new perspective allows us to derive and to understand the characteristic features of this integrator on a rather deep level.

In the next section I review the derivation of Hamilton's equations from the action expressed in Hamiltonian form. In Sec. III, I discretize the action and derive the VI equations from its extremum. In Sec. IV I show that the variational integrator is symplectic, and Noether's theorem holds. I also show that the VI equations can be written as the midpoint rule applied to Hamilton's equations. Section V contains a discussion of energy. There, it is shown that the energy is well behaved because the VI equations exactly conserve the value of a phase space function that is close, in a sense to be discussed, to the Hamiltonian. Several examples are given in Sec. VI. These examples explore the energy behavior and the convergence properties of the midpoint rule as a variational integrator.

My goal is to investigate variational and symplectic integration techniques for constrained Hamiltonian systems. In the next paper in this series [13], I will apply these techniques to a class of simple constrained Hamiltonian systems, namely, parametrized Hamiltonian mechanics. These are ordinary Hamiltonian systems with the coordinates, momenta, and time expressed as functions of an arbitrary parameter. The theory is invariant under changes of the parameter, and this gauge invariance gives

rise to a constraint that enforces conservation of energy. In future papers I will apply VI techniques to field theories with gauge symmetries. In canonical form these theories are described as constrained Hamiltonian systems with constraints that are local functions in space.

## II. CONTINUUM MECHANICS

Let the index $a$ label pairs of canonically conjugate dynamical variables $x_a$ and $p_a$. The action is a functional of $x_a(t)$ and $p_a(t)$, given by

$$S[p, x] = \int_{t'}^{t''} dt[p_a \dot{x}_a - H(p, x, t)]. \tag{1}$$

Here, $H(p, x, t)$ is the Hamiltonian and $t$ is physical time. The dot denotes differentiation with respect $t$. The summation convention is used for repeated indices, so the expression $p_a \dot{x}_a$ includes an implied sum over $a$.

Variation of the action (1) yields

$$\delta S[p, x] = \int_{t'}^{t''} dt\left[\left(\dot{x}_a - \frac{\partial H}{\partial p_a}\right)\delta p_a + \left(-\dot{p}_a - \frac{\partial H}{\partial x_a}\right)\delta x_a\right] + p_a \delta x_a|_{t'}^{t''}. \tag{2}$$

With the coordinates $x_a$ fixed at the initial and final times, $t'$ and $t''$, the endpoint terms in $\delta S$ vanish. Then the condition that the action should be stationary, $\delta S = 0$, yields

$$\dot{x}_a = \frac{\partial H}{\partial p_a}, \tag{3a}$$

$$\dot{p}_a = -\frac{\partial H}{\partial x_a}, \tag{3b}$$

These are the familiar Hamilton's equations. An immediate consequence of these equations is that the Hamiltonian function $H(p, x, t)$ satisfies

$$\dot{H} = \frac{\partial H}{\partial t}. \tag{4}$$

If $H$ has no explicit $t$ dependence, then $\dot{H} = 0$. In this case $H$, the energy, is a constant of the motion.

## III. DISCRETE MECHANICS

Let us divide the time interval between $t'$ and $t''$ into $N$ equal subintervals, or "zones", labeled $n = 1, \ldots, N$. These zones are separated by nodes, which are labeled $n = 0, \ldots, N$. As seen in Fig. 1 the endpoints of zone $n$ are nodes $n - 1$ and $n$. The expression $t^n$ denotes the time at the $n$th node. Likewise, $x_a^n$ and $p_a^n$ denote the coordinates and momenta at the $n$th node. The timestep is $\Delta t = t^n - t^{n-1}$. In this paper I consider the following second-order accurate discretization of the action (1):

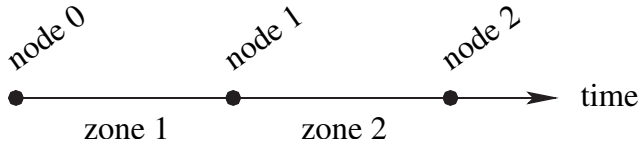


FIG. 1. Discretization in time. The nodes are labeled $n = 0, \ldots, N$ and the zones (or time intervals) are labeled $n = 1, \ldots, N$. The coordinates and momenta are node-centered, the Hamiltonian function is zone-centered.

$$S[p, x] = \sum_{n=1}^{N} \Delta t\left[p_a^{\underline{n}} \frac{\Delta x_a^n}{\Delta t} - H(p^{\underline{n}}, x^{\underline{n}}, t^{\underline{n}})\right]. \tag{5}$$

The $\Delta$ notation and the underlined index notation are employed repeatedly below; they are defined by

$$\Delta x_a^n \equiv x_a^n - x_a^{n-1}, \tag{6a}$$

$$x_a^{\underline{n}} \equiv \frac{x_a^n + x_a^{n-1}}{2}. \tag{6b}$$

These operations commute; that is, $x_a^{\underline{n}} - x_a^{\underline{n-1}} = (\Delta x_a^n + \Delta x_a^{n-1})/2$.

It will also prove useful to denote the value of the Hamiltonian in the $n$th zone by

$$H^n \equiv H(p^{\underline{n}}, x^{\underline{n}}, t^{\underline{n}}). \tag{7}$$

That is, we view $t$, $x_a$, and $p_a$ as node-centered in time and $H$ as zone-centered in time. [See Fig. 1.] Then Eq. (7) expresses the fact that, to second-order accuracy, the zone-centered values of $t$, $x_a$, and $p_a$ that appear in $H^n$ can be obtained from the averages of the neighboring node-centered values.

The discrete "Lagrangian", that is, the term in square brackets in Eq. (5), has truncation errors that scale like $\mathcal{O}(\Delta t^2)$. The discrete action is a sum over $N \sim 1/\Delta t$ terms, each having errors of order $\mathcal{O}(\Delta t^3)$. It follows that the error in $S$ typically scales like $\mathcal{O}(\Delta t^2)$. Thus the action (5) is second-order accurate. Note that Eq. (5) is not the only possible second-order discretization of the action. For pedagogical purposes, I have chosen to restrict considerations in this paper to the discrete action (5). Other discretizations, including some with higher order accuracy, will be discussed elsewhere [13].

Note that the momentum variables appear in the action (5) only in the combination $p_a^{\underline{n}} \equiv (p_a^n + p_a^{n-1})/2$. This combination represents the zone-centered momentum, accurate to second-order. Let us set this observation aside for the moment and treat the action as a function of all node-centered coordinates and momenta, $x_a^n$ and $p_a^n$ for $n = 0, \ldots, N$. The variation of $S$ is

$$\delta S = \sum_{n=1}^{N-1} \Delta t \left[ \frac{\Delta x_a^{n+1}}{\Delta t} - \left( \frac{\partial H}{\partial p_a} \right)^{n+1} \right] \delta p_a^n + \sum_{n=1}^{N-1} \Delta t \left[ -\frac{\Delta p_a^{n+1}}{\Delta t} - \left( \frac{\partial H}{\partial x_a} \right)^{n+1} \right] \delta x_a^n + \frac{1}{2} \left[ \Delta x_a^1 - \left( \frac{\partial H}{\partial p_a} \right)^1 \Delta t \right] \delta p_a^0 + \frac{1}{2} \left[ \Delta x_a^N - \left( \frac{\partial H}{\partial p_a} \right)^N \Delta t \right] \delta p_a^N - \left[ p_a^{\frac{1}{2}} + \frac{1}{2} \left( \frac{\partial H}{\partial x_a} \right)^1 \Delta t \right] \delta x_a^0 + \left[ p_a^{\frac{N}{2}} - \frac{1}{2} \left( \frac{\partial H}{\partial x_a} \right)^N \Delta t \right] \delta x_a^N. \tag{8}$$

Here and below we treat the derivatives of $H(p, x, t)$, like $H$ itself, as zone-centered quantities. Recall the notation defined in Eqs. (6) and (7). For any zone-centered function $F(p, x, t)$ of the canonical variables and time, we have $F^{\underline{n+1}} \equiv [F^{n+1} + F^n]/2 \equiv [F(p^{\underline{n+1}}, x^{\underline{n+1}}, t^{\underline{n+1}}) + F(p^{\underline{n}}, x^{\underline{n}}, t^{\underline{n}})]/2$. These notational rules apply to the derivatives of the Hamiltonian that appear in $\delta S$.

If we fix the coordinates at the endpoints, $x_a^0$ and $x_a^N$, then the condition that the discrete action should be extremized is

$$\frac{\Delta x_a^{\underline{n+1}}}{\Delta t} = \left( \frac{\partial H}{\partial p_a} \right)^{\underline{n+1}}, \qquad n = 1, \ldots, N-1, \tag{9a}$$

$$\frac{\Delta p_a^{\underline{n+1}}}{\Delta t} = -\left( \frac{\partial H}{\partial x_a} \right)^{\underline{n+1}}, \qquad n = 1, \ldots, N-1, \tag{9b}$$

$$\frac{\Delta x^1}{\Delta t} = \left( \frac{\partial H}{\partial p_a} \right)^1 \tag{9c}$$

$$\frac{\Delta x^N}{\Delta t} = \left( \frac{\partial H}{\partial p_a} \right)^N. \tag{9d}$$

These equations are redundant. For example, Eq. (9d) can be derived from Eqs. (9a) and (9c). This redundancy is a result of the fact that the action does not depend on the node-centered momenta $p_a^n$ independently, but only on the zone-centered combinations $p_a^{\underline{n}}$. We can combine Eqs. (9a), (9c), and (9d) into a single expression and write the equations of motion (9) as

$$\frac{\Delta x_a^{n+1}}{\Delta t} = \left( \frac{\partial H}{\partial p_a} \right)^{n+1}, \qquad n = 0, \ldots, N-1, \tag{10a}$$

$$\frac{\Delta p_a^{\underline{n+1}}}{\Delta t} = -\left( \frac{\partial H}{\partial x_a} \right)^{\underline{n+1}}, \qquad n = 1, \ldots, N-1. \tag{10b}$$

The equations of motion in this form can be obtained directly from the action (5) by extremizing with respect to the node-centered coordinates $x_a^n$ and the zone-centered momenta $p_a^{\underline{n}}$. They are a discrete form of Hamilton's Eqs. (3).

The equations of motion (10) constitute the variational integrator defined by the discrete action (5). Since they are derived from a variational principle, these equations naturally define a boundary value problem in which the freely chosen data are divided between the endpoints in time. Thus, given the boundary data $x_a^0$ and $x_a^N$, Eqs. (10) determine the coordinates $x_a^n$ for $n = 1, \ldots, N-1$ and momenta $p_a^{\underline{n}}$ for $n = 1, \ldots, N$. We can add boundary terms to the action to change the permitted boundary conditions. However, in practice, our primary interest is not in any of these boundary value problems. Rather, we are interested in solving an initial value problem. Thus, we are faced with the task of reinterpreting the equations of motion in such a way that initial data can be posed and evolved into the future.

It is not difficult to reinterpret the variational integrator (10) as an initial value problem. One possibility is to choose values for the coordinates at the initial time $t^0$ and values for the momenta at the half timestep $t^{\underline{1}}$; that is, we choose $x_a^0$ and $p_a^{\frac{1}{2}}$. Then Eq. (10a) with $n = 0$ can be solved for $x_a^1$. This completes the determination of data at "levels" $n = 0$ and 1. Alternatively, we can generate data at levels $n = 0$ and 1 by specifying $x_a^0$ and $x_a^1$, then solving Eq. (10a) with $n = 0$ for $p_a^{\frac{1}{2}}$. Once the data at levels 0 and 1 have been found, we can solve Eqs. (10) with $n = 1$ for the level 2 data $x_a^2$, and $p_a^{\frac{2}{2}}$. We continue in this fashion to obtain the data at levels 3, 4, etc.

Strictly speaking, neither of the options outlined above is an *initial* value problem. With the first option, the freely specifiable data $x_a^0$, $p_a^{\frac{1}{2}}$ are split between the initial time node and the first time zone. With the second option, the data $x_a^0$ and $x_a^1$ are split between time nodes 0 and 1. Apart from this slight misuse of the word "initial", we see that it is fairly trivial to reinterpret the variational integrator equations (10) as an initial value problem. With higher order discretizations, this reinterpretation is not so simple [13].

## IV. SYMPLECTIC FORM, NOETHER'S THEOREM AND THE MIDPOINT RULE

In this section we show that the variational integrator (10) is symplectic, and that Noether's theorem applies. These results are derived in mathematically precise language for the Lagrangian formulation of mechanics by Marsden *et al.* [10,11]. In the process of developing these results, we show that the VI equations can be expressed in terms of the node-centered momentum. The discrete equations are equivalent to the midpoint rule applied to Hamilton's equations.

Consider first the continuous Hamiltonian system defined by the action (1). The canonical two-form is defined by

$$\omega = dp_a \wedge dx_a, \tag{11}$$

where $d$ is the exterior derivative and $\wedge$ is the exterior product. Hamiltonian systems are symplectic, meaning that the form $\omega$ is invariant under time evolution. We can derive this result by noting that, for a solution of the classical equations of motion (3), the variation of the action

reduces to the endpoint terms in Eq. (2). Let $S(x'', t''; x', t')$ denote the action evaluated along the classical history with endpoint data $x_a(t') = x'_a$ and $x_a(t'') = x''_a$. We see that $\partial S(x'', t''; x', t')/\partial x''_a = p_a(t'')$, and $\partial S(x'', t''; x', t')/\partial x'_a = -p_a(t')$. Then the exterior derivative of the action is given by

$$dS(x'', t''; x', t') = p_a dx_a|_{t'}^{t''}, \tag{12}$$

where $p_a$ is the canonical momentum evaluated along the classical path. The identity $ddS(x'', t''; x', t') = 0$ shows that $dp_a \wedge dx_a|_{t'}^{t''}$ vanishes, so that $\omega$ is constant in time.

Now turn to the discrete system defined by the action (5). Let us define the coefficient of $\delta x_a^N$ that appears in $\delta S$ [Eq. (8)] as ${}^{(-)}\mathcal{P}_a^N$, where

$${}^{(-)}\mathcal{P}_a^n \equiv p_a^{\underline{n}} - \frac{\Delta t}{2}\left(\frac{\partial H}{\partial x_a}\right)^n. \tag{13}$$

Similarly, we can define the coefficient of $\delta x_a^0$ as ${}^{(+)}\mathcal{P}_a^0$, where

$${}^{(+)}\mathcal{P}_a^n \equiv p_a^{\underline{n+1}} + \frac{\Delta t}{2}\left(\frac{\partial H}{\partial x_a}\right)^{n+1}. \tag{14}$$

The VI equations (10) define an evolution in phase space. Obviously this evolution can be extended to values of $n$ beyond nodes 0 and $N$. Likewise, we can apply our definitions of ${}^{(-)}\mathcal{P}_a^n$ and ${}^{(+)}\mathcal{P}_a^n$ for all integer $n$. Now observe that the VI equations imply that ${}^{(+)}\mathcal{P}_a^n - {}^{(-)}\mathcal{P}_a^n$ vanishes when the extended equations of motion hold. Thus, we can drop the superscripts $(+)$ and $(-)$ and denote both ${}^{(+)}\mathcal{P}_a^n$ and ${}^{(-)}\mathcal{P}_a^n$ by $\mathcal{P}_a^n$.

Let $S(x^N, t^N; x^0, t^0)$ denote the value of the discrete action (5) for a solution of the VI equations of motion with endpoint data $x_a^N$ at $t^N$ and $x_a^0$ at $t^0$. The variation in Eq. (8) shows that, when the (extended) equations of motion hold,

$$dS(x^N, t^N; x^0, t^0) = \mathcal{P}_a^n dx_a^n|_{n=0}^N. \tag{15}$$

This is the analog of Eq. (12) above. Taking the exterior derivative of this expression we find

$$0 = d\mathcal{P}_a^n \wedge dx_a^n|_{n=0}^N. \tag{16}$$

Thus, the discrete action naturally defines a symplectic two-form

$$\omega = d\mathcal{P}_a^n \wedge dx_a^n \tag{17}$$

that is conserved under the phase space evolution defined by the VI equations of motion.

In the analysis above we defined

$$\mathcal{P}_a^{\underline{n}} = p_a^{\underline{n}} - \frac{\Delta t}{2}\left(\frac{\partial H}{\partial x_a}\right)^n = p_a^{\underline{n+1}} + \frac{\Delta t}{2}\left(\frac{\partial H}{\partial x_a}\right)^{n+1}. \tag{18}$$

The two expressions for $\mathcal{P}_a^n$ are equivalent when the equations of motion hold. A short calculation using Eq. (10b) shows that

$$\mathcal{P}_a^{\underline{n+1}} \equiv \frac{\mathcal{P}_a^{n+1} + \mathcal{P}_a^n}{2} = p_a^{\underline{n+1}}. \tag{19}$$

Therefore we see that, when the equations of motion hold, $\mathcal{P}_a^n$ can be identified as the node momentum $p_a^n$.

The equation of motion for $\mathcal{P}_a^n$ can be derived by computing $\Delta\mathcal{P}_a^n$ and using the VI equation (10b). Along with Eq. (10a), we have

$$\frac{\Delta x_a^{n+1}}{\Delta t} = \left(\frac{\partial H}{\partial p_a}\right)^{n+1}, \tag{20a}$$

$$\frac{\Delta \mathcal{P}_a^{n+1}}{\Delta t} = -\left(\frac{\partial H}{\partial x_a}\right)^{n+1}. \tag{20b}$$

This is perhaps the most elegant form of the VI equations. They are simply Hamilton's equations discretized with the midpoint rule. Their interpretation as an initial value problem is straightforward: given data $x_a^0$ and $\mathcal{P}_a^0$ at the initial time, we solve the equations with $n = 0$ for $x_a^1$, $\mathcal{P}_a^1$. Repeat to find data at nodes $n = 2, 3, \ldots$. Recall that the derivatives of $H$ that appear on the right-hand sides of Eqs. (20) are zone-centered functions. Thus, they are evaluated at $\mathcal{P}_a^{\underline{n+1}}$ $x_a^{\underline{n+1}}$, and $t^{\underline{n+1}}$.

Noether's theorem states that symmetries give rise to conserved "charges". We now show that when the discrete action is invariant under a symmetry transformation, there exists a charge that is exactly conserved by the VI equations.

Consider first the continuum case. Let $x_a \rightarrow X_a^\sigma(x)$ be a one-parameter family of transformations that leave the action, expressed in Lagrangian form, unchanged. Since we are working with the Hamiltonian formalism, let us extend this family of configuration space transformations to a family of point canonical transformations:

$$x_a \rightarrow X_a^\sigma, \tag{21a}$$

$$p_a \rightarrow P_a^\sigma \equiv p_b \frac{\partial X_b^{-\sigma}}{\partial x_a}. \tag{21b}$$

Here, it is assumed that $\sigma = 0$ coincides with the identity transformation. By differentiating the relation $x_a = X_a^{-\sigma}(X^\sigma(x))$ we see that $P_a^\sigma \dot{X}_a^\sigma = p_a \dot{x}_a$ so the transformation (21) is indeed canonical.

By assumption the action (1) is unchanged by the transformations (21), so we have $S[p, x] = S[P^\sigma, X^\sigma]$ for all $\sigma$. It follows that the derivative of $S[P^\sigma, X^\sigma]$ with respect to $\sigma$ must vanish. On the other hand, the endpoint terms in the general variation of the action (2) imply that, if $X_a^\sigma$, $P_a^\sigma$ satisfy the equations of motion when $\sigma = 0$, then

$$\frac{dS[P^\sigma, X^\sigma]}{d\sigma} = p_a \frac{dX_a^\sigma}{d\sigma}\Bigg|_{t'}^{t''} \tag{22}$$

at $\sigma = 0$. Because the left-hand side of this equation vanishes, we see that the charge

$$Q \equiv p_a \frac{dX_a^\sigma}{d\sigma}\bigg|_{\sigma=0} \tag{23}$$

is conserved in time for the classical motion of the system.

Now turn to the discrete case. Let us assume that the discrete action (5) is unchanged when the variables $x_a^n$, $p_a^n$ are transformed by Eqs. (21) for each value of $n$. Then, as in the continuum case, the derivative of $S[P^\sigma, X^\sigma]$ with respect to $\sigma$ vanishes. The general variation of the action (8) implies that, if $(X_a^\sigma)^n$, $(P_a^\sigma)^n$ satisfy the equations of motion at $\sigma = 0$, then

$$\frac{dS[P^\sigma, X^\sigma]}{d\sigma} = \mathcal{P}_a^n \frac{d(X_a^\sigma)^n}{d\sigma}\bigg|_{n=0}^{N} \tag{24}$$

at $\sigma = 0$. Here, I have used the definitions (18) for $\mathcal{P}_a^n$. Since the left-hand side of this relationship vanishes, we find that the charge

$$Q \equiv \mathcal{P}_a^n \frac{d(X_a^\sigma)^n}{d\sigma}\bigg|_{\sigma=0} \tag{25}$$

is conserved (independent of $n$) by the VI equations (10) or (20).

## V. ENERGY CONSERVATION

One of the key characteristics of variational integrators that makes them interesting and important is their behavior with respect to energy. If the Hamiltonian has no explicit time $t$ dependence then the energy is conserved in the continuum theory; see Eq. (4). Variational integrators do not conserve energy exactly, but typically the energy error does not grow as the evolution time increases. To be precise, in this section I show that the VI equations (20) exactly conserve the value of a phase space function $\mathcal{H}$ that differs from the Hamiltonian $H$ by terms of order $\mathcal{O}(\Delta t^2)$. The coefficient of the $\mathcal{O}(\Delta t^2)$ difference is a phase space function that remains bounded at least as long as the solution trajectory is bounded in phase space. It follows that the value of energy predicted by the VI equations will be ''close'' to the exact value, where close means that the error is of order $\mathcal{O}(\Delta t^2)$ with a coefficient that does not exhibit unbounded growth in time.

Let us begin the analysis by considering the continuum evolution for a system with time-independent Hamiltonian $\mathcal{H}(p, x)$. This system is described by the action

$$S[p, x] = \int_{t'}^{t''} dt[p_a \dot{x}_a - \mathcal{H}(p, x)], \tag{26}$$

with variation

$$\delta S = \text{eom's} + p_a \delta x_a|_{t'}^{t''}. \tag{27}$$

The terms listed as ''eom's'' are the terms that yield Hamilton's equations of motion. Let $S(x'', t''; x', t')$ denote the action (26) evaluated at the solution of Hamilton's equations with endpoint data $x_a'$ at $t'$ and $x_a''$ at $t''$. The variation equation (27) implies that $S(x'', t''; x', t')$ satisfies

$$\frac{\partial S(x'', t''; x', t')}{\partial x_a''} = p'', \tag{28a}$$

$$\frac{\partial S(x'', t''; x', t')}{\partial x_a'} = -p', \tag{28b}$$

where $p_a' = p_a(t')$ and $p_a'' = p_a(t'')$. These equations show that $-S(x'', t''; x', t')$ is a Type 1 generating function for a canonical transformation from ''old'' coordinates and momenta $x_a'$, $p_a'$ to ''new'' coordinates and momenta $x_a''$, $p_a''$ [24]. We also know that, starting from the initial data $x_a'$, $p_a'$, the classical trajectory generated by the Hamiltonian $\mathcal{H}(p, x)$ passes through the phase space point $x_a''$, $p_a''$. Thus, $-S(x'', t''; x', t')$ is a Type 1 generating function that generates a canonical transformation representing the time evolution of the system from $t'$ to $t''$.

Generating functions of different type are related by functions of the old and new coordinates and momenta. We can define a new generating function $H$ by

$$H \equiv \frac{p_a'' + p_a'}{2}\frac{x_a'' - x_a'}{t'' - t'} - \frac{S(x'', t''; x', t')}{t'' - t'}. \tag{29}$$

Eqs. (28) can be written as $dS(x'', t''; x', t') = p_a'' dx_a'' - p_a' dx_a'$. From this result it is straightforward to show that the exterior derivative of $H$ is given by

$$dH = \frac{\Delta x_a}{\Delta t} d\bar{p}_a - \frac{\Delta p_a}{\Delta t} d\bar{x}_a, \tag{30}$$

where $\bar{p}_a \equiv (p_a'' + p_a')/2$, $\bar{x}_a \equiv (x_a'' + x_a')/2$, $\Delta p_a \equiv p_a'' - p_a'$, $\Delta x_a \equiv x_a'' - x_a'$, and $\Delta t \equiv t'' - t'$. Thus, $H$ can be viewed as a function of $\bar{p}_a$ and $\bar{x}_a$. The canonical transformation that represents the classical evolution from $t'$ to $t''$ is written in terms of the new generating function $H \equiv H(\bar{p}, \bar{x})$ as

$$\frac{\partial H(\bar{p}, \bar{x})}{\partial \bar{p}_a} = \frac{\Delta x_a}{\Delta t}, \tag{31a}$$

$$\frac{\partial H(\bar{p}, \bar{x})}{\partial \bar{x}_a} = -\frac{\Delta p_a}{\Delta t}. \tag{31b}$$

These are precisely the VI equations (20), the midpoint rule, with some simple changes of notation.

The analysis above shows that the VI equations (20) can be viewed as the generating function equations for a canonical transformation from old coordinates and momenta $x_a^n$, $\mathcal{P}_a^n$ to new coordinates and momenta $x_a^{n+1}$, $\mathcal{P}_a^{n+1}$. The generating function is $H(\underline{\mathcal{P}^{n+1}}, \underline{x^{n+1}}, \Delta t)$; it is helpful at this point in the analysis to consider $H$ as dependent on the timestep $\Delta t$ as well as the coordinates and momenta. The canonical transformation generated by $H$ defines a mapping of phase space that coincides with the exact time evolution described by the Hamiltonian $\mathcal{H}(\mathcal{P}, x)$. The relationship between $H$ and $\mathcal{H}$ is given by

$$H(\mathcal{P}^{\underline{n+1}}, x^{\underline{n+1}}, \Delta t) = \mathcal{P}_a^{\underline{n+1}} \frac{\Delta x_a^{n+1}}{\Delta t} - \frac{S(x^{n+1}, t^{n+1}; x^n, t^n)}{\Delta t}. \tag{32}$$

This is Eq. (29) with appropriate changes in notation. The function $S(x^{n+1}, t^{n+1}; x^n, t^n)$ is the continuum action (26) evaluated at the solution of the equations of motion with endpoint data $x_a^n$ at $t^n$ and $x_a^{n+1}$ at $t^{n+1}$. Analogous to Eqs. (28), we have the relations

$$\mathcal{P}_a^{n+1} = \frac{\partial S(x^{n+1}, t^{n+1}; x^n, t^n)}{\partial x_a^{n+1}}, \tag{33a}$$

$$\mathcal{P}_a^{n} = -\frac{\partial S(x^{n+1}, t^{n+1}; x^n, t^n)}{\partial x_a^{n}}, \tag{33b}$$

that define the momenta at the endpoints.

The discrete evolution defined by the VI equations with Hamiltonian $H$ coincides with the exact continuum evolution defined by Hamilton's equations with Hamiltonian $\mathcal{H}$. Since the exact evolution conserves $\mathcal{H}$, it follows that the VI equations conserve $\mathcal{H}$. We now show by explicit calculation that $H$ and $\mathcal{H}$ differ by terms of order $\mathcal{O}(\Delta t^2)$.

In order to evaluate the action $S$ along the classical solution between $t^n$ and $t^{n+1}$, we first expand the solution $x_a(t)$, $p_a(t)$ in a series in $t$ with coefficients that depend on $x_a^{\underline{n+1}}$ and $p_a^{\underline{n+1}} \equiv \mathcal{P}_a^{\underline{n+1}}$. The calculation is simplified by writing Hamilton's equations (3) as

$$\dot{\xi}_a = \omega_{ab} \mathcal{H}_b, \tag{34}$$

where $\xi_a$ denotes the set of canonical variables $\{x_a, p_a\}$ and $\omega_{ab}$ is the matrix

$$\omega_{ab} = \begin{pmatrix} 0 & -I \\ I & 0 \end{pmatrix}. \tag{35}$$

Here and below, subscripts on $\mathcal{H}$ denote derivatives;, for example, $\mathcal{H}_b \equiv \partial \mathcal{H} / \partial \xi_b$. The solution is

$$\xi_a(t) = \xi_a^{\underline{n+1}} + \omega_{aa'}[\mathcal{H}_{a'} + \mathcal{H}_{a'bc}\omega_{bb'}\mathcal{H}_{b'}\omega_{cc'}\mathcal{H}_{c'}\Delta t^2/8](t - t^{\underline{n+1}}) + \tfrac{1}{2}\omega_{aa'}\mathcal{H}_{a'b}\omega_{bb'}\mathcal{H}_{b'}[(t - t^{\underline{n+1}})^2 - (\Delta t^{n+1})^2/4] + \tfrac{1}{24}\omega_{aa'}[\mathcal{H}_{a'bc}\omega_{bb'}\mathcal{H}_{b'}\omega_{cc'}\mathcal{H}_{c'} + \mathcal{H}_{a'b}\omega_{bb'}\mathcal{H}_{b'c}\omega_{cc'}\mathcal{H}_{c'}][4(t - t^{\underline{n+1}})^3 - 3(t - t^{\underline{n+1}}) \times (\Delta t^{n+1})^2] + \mathcal{O}(\Delta t^4), \tag{36}$$

where all derivatives of $\mathcal{H}$ are evaluated at $\xi_a^{\underline{n+1}}$.

The Type I generating function $-S(x^{n+1}, t^{n+1}; x^n, t^n)$ is written as a function of $\xi_a^{\underline{n+1}}$ by inserting the solution (36) into the action (26), with initial and final times $t^n$ and $t^{n+1}$. The new generating function $H$ is then found from Eq. (32), with the result

$$H = \mathcal{H} + \tfrac{1}{24}\mathcal{H}_{ab}\omega_{aa'}\mathcal{H}_{a'}\omega_{bb'}\mathcal{H}_{b'}\Delta t^2 + \mathcal{O}(\Delta t^4). \tag{37}$$

Clearly, this formal expansion for $H$ in terms of $\mathcal{H}$ can be inverted to yield

$$\mathcal{H} = H - \tfrac{1}{24}H_{ab}\omega_{aa'}H_{a'}\omega_{bb'}H_{b'}\Delta t^2 + \mathcal{O}(\Delta t^4). \tag{38}$$

This is the desired relationship between the phase space functions $\mathcal{H}$ and $H$.

With the solution $\xi_a(t)$ expanded to terms of order $\Delta t^3$ in Eq. (36), the evaluation of Eq. (32) yields $H$ through terms of order $\Delta t^2$. However, a simple argument can be given to show that the terms of order $\Delta t^3$, and in fact all terms proportional to odd powers of $\Delta t$, must vanish. Consider Eq. (32), but let the data $t^n$, $x_a^n$ and $t^{n+1}$, $x_a^{n+1}$ exchange roles. The data must be exchanged in the definitions (33) as well; this yields

$$\mathcal{P}_a^{n} = \frac{\partial S(x^n, t^n; x^{n+1}, t^{n+1})}{\partial x_a^{n}}, \tag{39a}$$

$$\mathcal{P}_a^{n+1} = -\frac{\partial S(x^n, t^n; x^{n+1}, t^{n+1})}{\partial x_a^{n+1}}. \tag{39b}$$

Now, the function $S(x^n, t^n; x^{n+1}, t^{n+1})$ is just the action evaluated at the solution of Hamilton's equations with endpoint data $x_a(t^n) = x_a^n$ and $x_a(t^{n+1}) = x_a^{n+1}$. It differs from $S(x^{n+1}, t^{n+1}; x^n, t^n)$ only because the limits of integration are reversed. Hence, we have

$$S(x^n, t^n; x^{n+1}, t^{n+1}) = -S(x^{n+1}, t^{n+1}; x^n, t^n), \tag{40}$$

and we find that the definitions (39) are identical to Eqs. (33). It follows that the right-hand side of Eq. (32) is unchanged when we exchange the endpoint data. Equating the left-hand sides leads to

$$H(\mathcal{P}^{\underline{n+1}}, x^{\underline{n+1}}, \Delta t) = H(\mathcal{P}^{\underline{n+1}}, x^{\underline{n+1}}, -\Delta t). \tag{41}$$

Therefore, $H$ is an even function of $\Delta t$, and its expansion (37) in terms of $\mathcal{H}$ does not contain odd powers of $\Delta t$.

To summarize, the VI equations exactly conserve $\mathcal{H}$ and the Hamiltonian $H$ differs from $\mathcal{H}$ by terms of order $\Delta t^2$. The coefficient of the $\mathcal{O}(\Delta t^2)$ and higher order terms are constructed from derivatives of $H$. As long as the motion in phase space remains bounded, and the Hamiltonian and its derivatives are nonsingular, then these coefficients will remain bounded. It follows that $H$ will remain close to $\mathcal{H}$, which is constant, for all time. If the

motion in phase space does not remain bounded, it does not necessarily follow that the coefficient of the $\mathcal{O}(\Delta t^2)$ will grow in time. In this situation the results depend on the details of the Hamiltonian.

The energy behavior of the VI equations is quite different from the behavior exhibited by many numerical integrators. For example, second-order Runge-Kutta (RK2) typically exhibits errors in $H$ of order $\Delta t^2$ on short time scales and a drift in the value of $H$ of order $\Delta t^3$ on long-time scales. Fourth order Runge-Kutta (RK4) exhibits errors in $H$ of order $\Delta t^4$ on short time scales and a drift in $H$ of order $\Delta t^5$ on long-time scales. For both RK2 and RK4, the energy error becomes unboundedly large as time increases. We will see examples of these behaviors in the next section.

## VI. EXAMPLES

The examples in this section show the results obtained from numerical integration of simple Hamiltonian systems using the VI equations (20) and standard second and fourth order Runge–Kutta. Issues of efficiency are ignored. Clearly the midpoint rule, being implicit, is numerically more expensive to solve than explicit integration schemes. However, the aim of this paper is to investigate the properties of variational-symplectic integrators without concern for details of implementation. This is because, ultimately, we would like to apply these methods to theories like general relativity for which standard integration techniques are inadequate. The main goal, then, is to find a numerical algorithm that works—efficiency is at most a secondary concern.

One can solve the implicit VI equations using a Newton-Raphson method. But in practice it is much simpler and more reliable to iterate the equations until the answer is unchanged to a prescribed level of accuracy. Thus, given $x_a^n$ and $\mathcal{P}_a^n$, we begin the first iteration with the approximation $x_a^{n+1} \approx x_a^n$, $\mathcal{P}_a^{n+1} \approx \mathcal{P}_a^n$. This is inserted into the right-hand sides of the VI equations to yield improved approximations for $x_a^{n+1}$ and $\mathcal{P}_a^{n+1}$. The whole process is repeated until the desired level of accuracy is achieved. For the higher resolution runs presented below, about 5 iterations were needed to reach a solution that was accurate to 1 part in $10^{13}$. For the lower resolution runs, around 15 iterations were needed to reach this same level of accuracy.

### A. Coupled harmonic oscillators

Our first example is the system of coupled harmonic oscillators with Hamiltonian

$$H = \tfrac{1}{2}(p_x^2 + p_y^2) + \tfrac{1}{2}(x^2 + y^2) + \tfrac{1}{5}(x - y)^6. \qquad (42)$$

The graph in Fig. 2 shows the amplitude of one of the oscillators, $x$, as a function of time. The behavior exhibited is rather complicated. The two solid curves show the results of numerical integration with the VI equations (20)

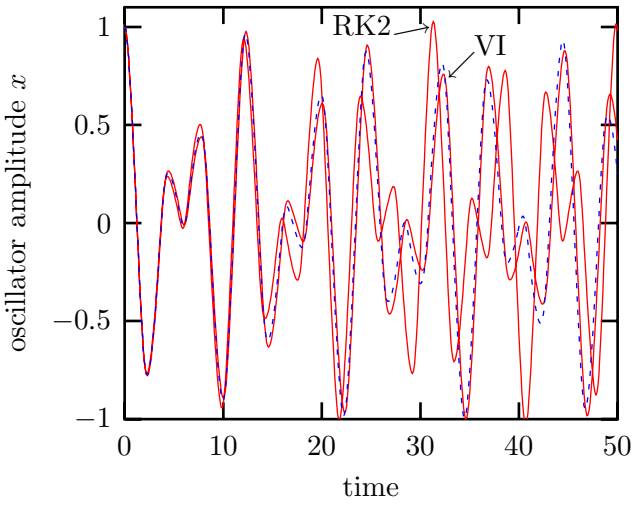


FIG. 2 (color online). The amplitude $x$ for the coupled harmonic oscillator as a function of time. The VI simulation produces the solid curve that tracks the exact solution (dashed curve) fairly closely. The other solid curve is obtained from RK2.

and second-order Runge-Kutta (RK2), both using a timestep of $\Delta t = 0.1$. The dashed curve is obtained from a fourth order Runge-Kutta integrator with timestep $\Delta t = 0.01$. Over the short time scale ($t \leq 50$) shown in the figure, the dashed curve can be taken as the "exact" solution. Compared to RK2, VI does a visibly better job of tracking the solution.

The initial data chosen for the coupled oscillator is $x = 1$, $y = p_x = p_y = 0$, so the exact solution has energy $H = 0.7$. Figure 3 shows the error in energy for VI at two resolutions. The solid curve shows the error for $\Delta t = 0.01$ while the dashed curve shows the error divided by

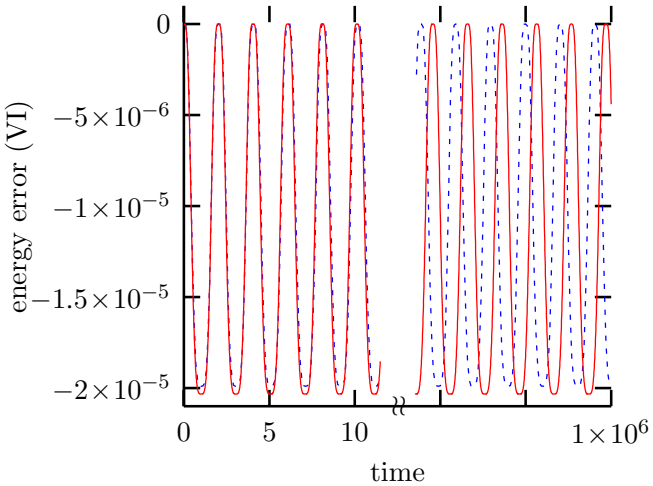


FIG. 3 (color online). Energy error for the coupled harmonic oscillator for VI. The solid curve has timestep $\Delta t = 0.01$. The dashed curve shows the error divided by 100 for $\Delta t = 0.1$. The results are displayed for the first and last ~12 time units; the total run time was $t = 1 \times 10^6$.

100 for $\Delta t = 0.1$. The close agreement between the amplitudes of these two curves shows that the energy error is second-order in the timestep. The key observation is that the energy error does not grow in time, even for the simulation with a relatively low resolution of $\Delta t = 0.1$.

The solid curve in Fig. 4 shows the energy error for RK2 at a resolution of $\Delta t = 0.01$. The dashed curve is the energy error for RK2 with resolution $\Delta t = 0.02$, divided by 8. Note that the two curves in this figure coincide on long-time scales ($t \gtrsim 5$). This shows that the drift in energy is order $\Delta t^3$. The short time scale errors are $\mathcal{O}(\Delta t^2)$, so the "wiggles" in the low resolution simulation (having been divided by 8) are approximately half the size of the wiggles seen in the high resolution run. For this particular system, and this particular choice of initial data, the growth rate of the energy error with RK2 is about $2.5\Delta t^3$ energy units per time unit.

Qualitatively similar results are found for RK4. In Fig. 5 the solid and dashed curves are obtained from simulations with timesteps $\Delta t = 0.01$ and 0.02, respectively. The errors for the low resolution case have been divided by 32. We see that the long-time scale drift in energy is $\mathcal{O}(\Delta t^5)$, while the short time scale wiggles are $\mathcal{O}(\Delta t^4)$. For this simulation the growth rate of the energy error is about $-1.1\Delta t^5$ energy units per time unit.

The value of energy $H$ obtained from VI is nearly constant because the VI equations exactly conserve the nearby Hamiltonian $\mathcal{H}$. This can be confirmed by computing the first two terms in the expansion for $\mathcal{H}$ given in Eq. (38). For the coupled harmonic oscillator with timestep $\Delta t = 0.01$, the two–term approximation for $\mathcal{H}$ remains nearly constant with variations at the level of $10^{-9}$. With timestep $\Delta t = 0.1$, the approximation for $\mathcal{H}$ remains nearly constant with variations at the level of $10^{-5}$.

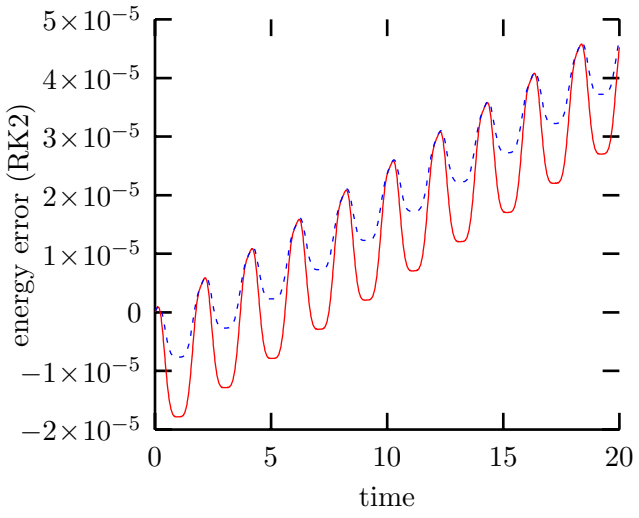


FIG. 4 (color online). Energy error for the coupled harmonic oscillator for RK2. The solid curve has timestep $\Delta t = 0.01$. The dashed curve shows the error divided by 8 for $\Delta t = 0.02$.

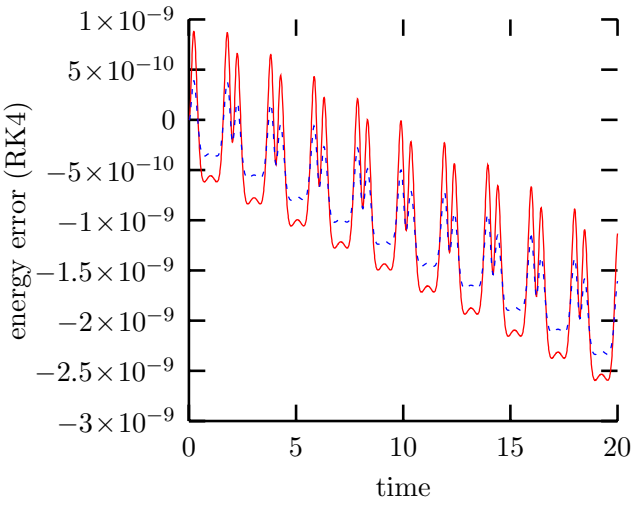


FIG. 5 (color online). Energy error for the coupled harmonic oscillator for RK4. The solid curve has timestep $\Delta t = 0.01$. The dashed curve shows the error divided by 32 for $\Delta t = 0.02$.

These variations are just what we expect given the fact that, according to Eq. (38), the terms omitted in the approximation for $\mathcal{H}$ are order $\mathcal{O}(\Delta t^4)$.

### B. Simple pendulum

For our next example, consider the simple pendulum with Hamiltonian

$$H = \tfrac{1}{2}p^2 - \cos(x), \tag{43}$$

where $x$ denotes the angle from the vertical and $p$ is the angular momentum. Figure 6 shows a portion of the phase space for the system. We consider a family of initial data points clustered about $x = \pi/2$, $p = 0$. Specifically, the initial data are given by

$$x = \pi/2 + 0.002\cos(\theta), \qquad p = 0.002\sin(\theta), \tag{44}$$

for $0 \le \theta \le 2\pi$. These points form a "circle" in phase

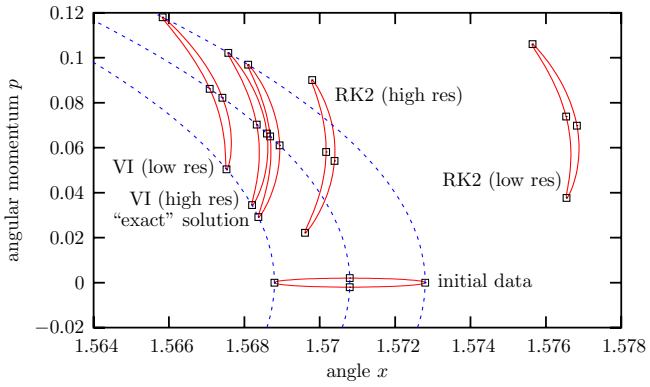


FIG. 6 (color online). Phase space diagram for the pendulum. The initial data occupy a circle around $x = \pi/2$, $p = 0$, and are evolved for just under 10 oscillation periods. Final data is shown for VI and RK2, for low and high resolutions.

space. The boxes in Fig. 6 mark the points $\theta = 0$, $\pi/2$, $\pi$, and $3\pi/2$. The initial data are evolved with VI and with RK2, both at low resolution (timestep $\Delta t = 0.1$) and high resolution (timestep $\Delta t = 0.05$). The run time is 74.1 time units, which is just under 10 oscillation periods. The initial data cycles around the phase space diagram in a clockwise direction. Figure 6 shows the end result of this evolution for the two integrators at low and high resolutions, as well as the exact solution obtained from RK4 with a very small timestep. The dashed curves show the constant energy contours with energies determined by the initial data shown as boxes.

Qualitatively, we see that both VI and RK2 schemes are second-order accurate. That is, the errors in $x$ and $p$ are reduced by a factor of about 4 when the resolution is doubled. But the character of that error is very different. The VI evolution stays close to the constant energy contours, and the phase space errors lie almost entirely in the $H =$ constant subspace. The RK2 integrator does not respect conservation of energy, and over time the system point in phase space spirals outward with increasing energy. After about 9000 time units the simulation with RK2 and $\Delta t = 0.1$ predicts that the pendulum will gain enough energy to circle around completely, rather than oscillate.

Recall that the midpoint rule is a symplectic integrator, that is, the symplectic form (17) is preserved in time. It follows that the volume of phase space bounded by the initial data circle in Fig. 6 is constant under the discrete evolution defined by the variational integrator. The standard second-order Runge-Kutta scheme is not symplectic, and does not preserve phase space volume. In Fig. 6 it is not possible to tell, simply by looking, whether or not the initial phase space volume is conserved by the VI scheme, or changed by the RK2 scheme. A more involved numerical test would be needed to verify the expected results.

### C. Unbounded motion in one dimension

The VI equations conserve the phase space function $\mathcal{H}$ exactly, but the energy $H$ might not remain close to $\mathcal{H}$ if the motion of the system is unbounded. Consider the Hamiltonian for a particle moving in a one-dimensional potential, $H = p^2/2 + V(x)$. In this case Eq. (38) gives

$$H - \mathcal{H} = \frac{\Delta t^2}{24}[p^2 V'' + (V')^2] + \mathcal{O}(\Delta t^4), \qquad (45)$$

where prime denotes $d/dx$. The time derivative of this difference is $d(H - \mathcal{H})/dt = p^3 V''' \Delta t^2/24$ plus terms of higher order in $\Delta t$. We see that $H - \mathcal{H}$, and therefore also $H$, will grow in time if $p^3 V'''$ remains finite and does not change sign.

A nice example of this unbounded behavior is obtained with the potential $V(x) = -x^{6/5}$. In this case the particle motion at late times is given approximately by $x \sim (2\sqrt{2}t/5)^{5/2}$, $p \sim \sqrt{2}(2\sqrt{2}t/5)^{3/2}$. Equation (45) shows that the energy grows linearly with time, $H \sim \mathcal{H} + (2\sqrt{2}\Delta t^2/125)t$. Figure 7 confirms that for this system, the variational integrator exhibits linear growth in the energy. The initial data used in this simulation was $x = 0.1$, $p = 0$, with timestep $\Delta t = 0.1$. The energy error obtained from RK2 is almost identical to the result shown in Fig. 7 for VI.

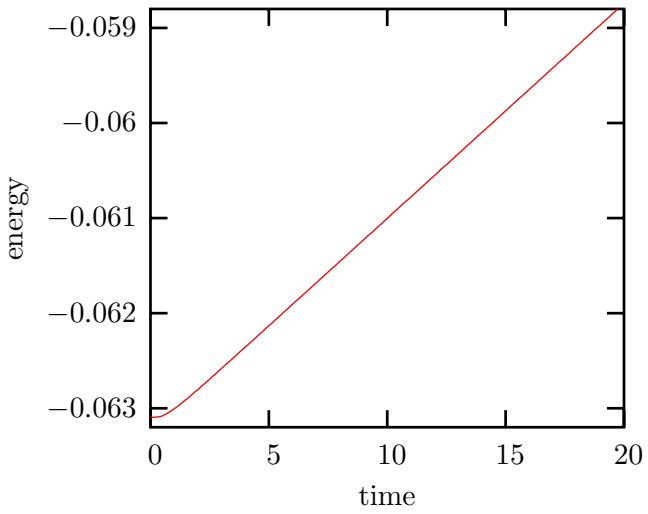


FIG. 7 (color online). Energy as a function of time for a particle in a one-dimensional potential, $V(x) = -x^{6/5}$, obtained with VI. As expected, the error in energy grows linearly with time.

### D. Orbital motion

Our final example is motion in a gravitational (or electric) field described by a central $1/r$ potential. The Hamiltonian is defined by

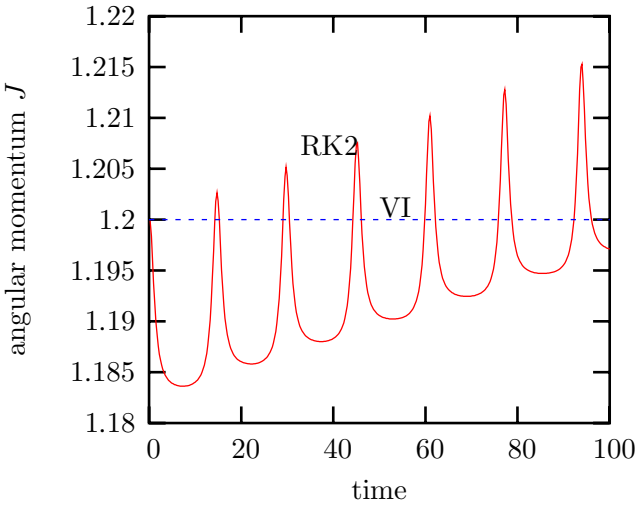


FIG. 8 (color online). Angular momentum as a function of time for motion in a central potential. The solid curve is obtained from RK2. The constant, dashed line is obtained with the variational integrator.

$$H = \frac{1}{2}(p_x^2 + p_y^2) - \frac{1}{\sqrt{x^2 + y^2}}. \quad (46)$$

This system is symmetric under rotations in the $x$–$y$ plane. The conserved Noether charge associated with rotational symmetry is angular momentum, $J \equiv x p_y - y p_x$. The initial data for this simulation is $x = 1.0$, $p_x = 0.0$, $y = 0.0$, $p_y = 1.2$. The resulting orbital motion is an ellipse with eccentricity $\sim 0.5$ and period $\sim 15$.

Figure 8 shows the angular momentum as a function of time for RK2 and VI with timestep $\Delta t = 0.25$. With the variational integrator the angular momentum is exactly conserved (to machine accuracy) and $J$ retains its initial value of 1.2 throughout the simulation. With RK2, the angular momentum exhibits short timescale fluctuations and a longer timescale drift. A more complete analysis shows that the short timescale errors are order $\Delta t^2$, whereas the drift in $J$ is order $\Delta t^3$. Qualitatively similar results are obtained for RK4. In that case, the short timescale errors in $J$ are order $\Delta t^4$, and the drift is order $\Delta t^5$.

## ACKNOWLEDGMENTS

This work was supported by NASA Space Sciences Grant No. ATP02–0043–0056.

[1] M. Henneaux and C. Teitelboim, *Quantization of Gauge Systems* (Princeton University Press, Princeton, 1992).
[2] P. Dirac, *Lectures on Quantum Mechanics* (Academic Press, Yeshiva University, New York, 1964).
[3] A. Taflove and S. Hagness, *Computational Electrodynamics: The Finite-Difference Time-Domain Method* (Artech House, Norwood, MA, 2005).
[4] B. Bruegmann, W. Tichy, and N. Jansen, Phys. Rev. Lett. **92**, 211101 (2004).
[5] L. E. Kidder, M. A. Scheel, S. A. Teukolsky, E. D. Carlson, and G. B. Cook, Phys. Rev. D **62**, 084032 (2000).
[6] L. E. Kidder, M. A. Scheel, and S. A. Teukolsky, Phys. Rev. D **64**, 064017 (2001).
[7] M. A. Scheel, L. E. Kidder, L. Lindblom, H. P. Pfeiffer, and S. A. Teukolsky, Phys. Rev. D. **66**, 124005 (2002).
[8] L. Lindblom *et al.*, Phys. Rev. D **69**, 124025 (2004).
[9] D. L. Meier, Astrophys. J. **595**, 980 (2003).
[10] J. E. Marsden and M. West, Acta Numerica **10**, 357 (2001).
[11] A. Lew, J. E. Marsden, M. Ortiz, and M. West, in *Finite Elements Methods: 1970's and Beyond*, edited by L. P. Franca, T. E. Tezduyar, and A. Masud (CIMNE, Barcelona, 2004).
[12] J. Sanz-Serna, Acta Numerica 243 (1991).
[13] J. D. Brown, to be published.
[14] R. Arnowitt, S. Deser, and C. W. Misner, gr-qc/0405109.
[15] J. W. York, Phys. Rev. Lett. **82**, 1350 (1999).
[16] H. P. Pfeiffer and J. W. York, Phys. Rev. D **67**, 044022 (2003).
[17] J. D. Brown, Phys. Rev. D **71**, 104011 (2005).
[18] C. Di Bartolo, R. Gambini, and J. Pullin, Classical Quantum Gravity **19**, 5275 (2002).
[19] R. Gambini and J. Pullin, Phys. Rev. Lett. **90**, 021301 (2003).
[20] R. Gambini and J. Pullin, Classical Quantum Gravity **20**, 3341 (2003).
[21] C. Di Bartolo, R. Gambini, and J. Pullin, J. Math. Phys. (N.Y.) **46**, 032501 (2005).
[22] R. Gambini and J. Pullin, gr-qc/0505023.
[23] R. Gambini and J. Pullin, gr-qc/0505052.
[24] H. Goldstein, C. Poole, and J. Safko, *Classical Mechanics* (Addison Wesley, San Francisco, 2002).